Neutron diffraction study of $GdBe_{13}$ magnetic structure

1982 J. Phys. F: Met. Phys. 12 223

(http://iopscience.iop.org/0305-4608/12/1/019)

J. Phys. F: Met. Phys., 12(1982)223-32. Printed in Great Britain

Neutron diffraction study of $GdBe_{13}$ magnetic structure

F Vigneron†, M Bonnet†, A Herr‡ and J Schweizer§
† CEN Saclay, BP No 2, 91190 Gif-Sur-Yvette, France
‡ Institut de Physique, Strasbourg, France
§ DRF/CENG and Institut Laue-Langevin, Grenoble, France

Received 9 February 1981, in final form 1 July 1981

Abstract. Neutron diffraction ($\lambda = 0.504$ Å) has been used to show that below $T_N = 27 \pm 3$ K, $GdBe_{13}$ exhibits a spiral structure. The propagation vector is parallel to c and independent of temperature. The magnetic moments M of the Gd^{3+} ions are perpendicular to the c axis. The thermal variation of M can be accounted for by means of a molecular field approximation ($J = 7/2$, $g_J = 2$).

1. Introduction

The rare-earth (RE) beryllides $REBe_{13}$ crystallise in the cubic $NaZn_{13}$-type structure, space group $Fm3c$, with: 8 RE in (a) ($\frac{1}{4}$ $\frac{1}{4}$ $\frac{1}{4}$) (cubic point group symmetry 43), 8 Be_I in (b) (0 0 0), and 96 Be_{II} in (i) (0 y z) with $y \simeq 0.114$ and $z \simeq 0.176$. Magnetic experiments on $REBe_{13}$ (Bucher *et al* 1975, Herr *et al* 1975) with RE = Gd, Tb, Dy, Ho and Er have shown an antiferromagnetic behaviour with Néel temperatures T_N obeying de Gennes' law.

Neutron diffraction experiments on $REBe_{13}$ (Vigneron *et al* 1980, Vigneron 1981) with RE = Tb, Dy, Ho and Er have revealed incommensurate and/or commensurate magnetic structures. For $T_N < T < T_N$, $TbBe_{13}$ and $HoBe_{13}$ exhibit an incommensurate spiral structure, with a propagation vector τ equal to $\frac{1}{3}c^*$ $(1 - \varepsilon(T))$ and magnetic moments perpendicular to the c axis. For these compounds the low-temperature magnetic structure observed at $T < T_N$, as well as the magnetic structure at $T < T_N$ for RE = Dy and Er, is a commensurate structure (magnetic cell (a, a, $3a$); moments are perpendicular to c).

These observed effects result from the competition between indirect exchange interactions and anisotropy. In as much as this kind of competition is absent in $GdBe_{13}$, due to its negligible magnetocrystalline anisotropy, it is obviously of interest to determine the magnetic structure of a material such as $GdBe_{13}$, for which exchange interactions play a dominant role.

2. Experimental procedure

2.1. Experimental conditions

The $GdBe_{13}$ sample was prepared by high-frequency induction melting in a BeO crucible, in a pure argon atmosphere, starting from 99.9% pure Gd and Be.

0305-4608/82/010223 + 10$01.50

The large absorption cross section of natural Gd for thermal neutrons ($\sigma_a \simeq 20\,000$ b at $\lambda \simeq 1$ Å) prevents detailed neutron diffraction studies. However experiments can be performed at a smaller wavelength (Morin *et al* 1978): $\sigma_a \simeq 800$ b at $\lambda \simeq 0.5$ Å. Measurements were carried out on a powder sample at the high flux reactor in Grenoble (D_4 spectrometer) with $\lambda = 0.504$ Å. The linear absorption coefficient, measured experimentally, was $\mu = 2.5\,\text{cm}^{-1}$. The sample holder was cylindrical with an 8 mm diameter. Several neutron diffraction patterns were obtained in the paramagnetic region ($T = 31$ K) and below T_N ($T = 20$ K, 12 K and 3 K).

2.2. *Profile refinement*

The powder patterns were refined by the profile analysis technique (Rietveld 1967, Hewat 1973) which minimises:

$$M = \sum_i w_i \left(y_i(\text{obs}) - \frac{1}{c} y_i(\text{calc}) \right)^2$$

where y_i(obs) and y_i(calc) are the observed and calculated intensities at any $2\theta_i$ of the diagram. The statistical weight w_i is proportional to $1/(y_i(\text{obs}) + \text{estimated background at } 2\theta_i)$ and c is a scale factor.

Although determination of the background is quite easy for the nuclear pattern at $T = 31$ K (figure 1), it is much more difficult at T lower than T_N (figures 2, 3 and 4) when nuclear and magnetic peaks cover the whole diagram. However, as the differences

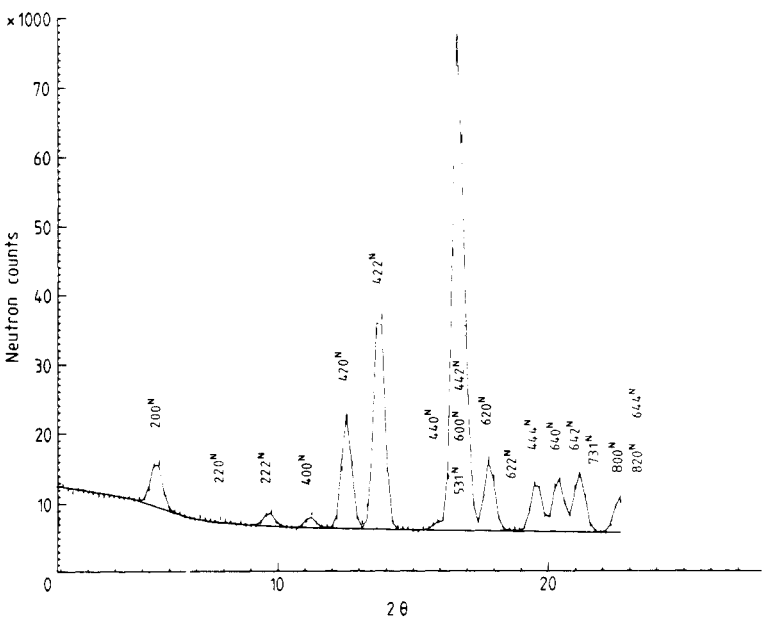

Figure 1. Profile refinement for crystalline structure ($T = 31$ K). In figures 1, 2, 3 and 4 the vertical lines indicate the experimental neutron counts and their accuracies, defined by counts $\pm 2\sqrt{\text{counts}}$. The upper full curve is the calculated profile and the lower full curve corresponds to diffuse background scattering. Bragg peaks are indexed in the (a, a, a) cubic cell.

between the background at $T < T_N$ and the background at $T = 31$ K are mainly due to paramagnetic scattering, we have taken:

$$\text{background } (T < T_N) = \text{background } (31 \text{ K}) - \alpha(T) f^2$$

where f is the magnetic form factor of Gd^{3+} and $\alpha(T)$ is a parameter to be refined in the Rietveld profile refinement program. The difference in diffuse scattering at temperatures above ($T = 31$ K) and below the ordering transition temperature T_N, $\alpha(T)f^2$, represents that part of the paramagnetic scattering which becomes ordered at low temperatures. Consequently $\alpha(T)$ is proportional to M^2, where M is the average atomic magnetic moment in the ordered magnetic lattice.

The results of the profile refinements (see tables 1 and 2) lead to

$$\alpha(T)/M^2 = \begin{cases} 31(4) & \text{at } T = 20 \text{ K} \\ 32(4) & \text{at } T = 12 \text{ K} \\ 32(2) & \text{at } T = 3 \text{ K}. \end{cases}$$

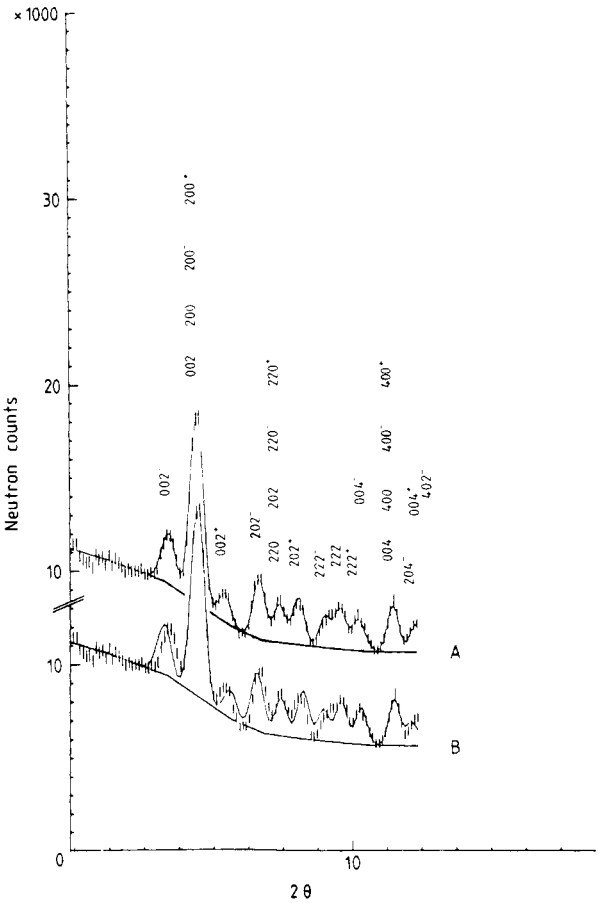

Figure 2. Profile refinement for magnetic structure ($T = 3$ K). The calculated profile corresponds either to an incommensurate magnetic structure with a propagation vector $\tau = 0.284\ c^*$ (curve A) or to a commensurate magnetic structure $\tau = \frac{1}{3}\ c^*$ (curve B). In both cases, nuclear (hkl) and magnetic ($hkl^{\pm}$) Bragg peaks are indicated in the (a, a, a) cubic cell.

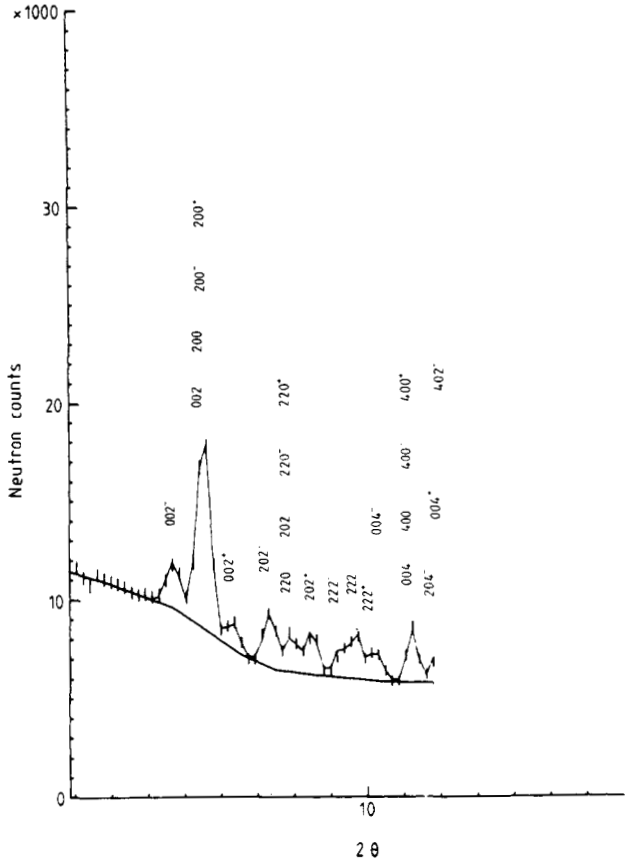

Figure 3. Profile refinement for magnetic structure ($T = 12$ K). The calculated profile (upper full curve) corresponds to an incommensurate magnetic structure with $\tau = 0.285\,c^*$. Nuclear (hkl) and magnetic ($hkl^{\pm}$) Bragg peaks are indexed in the (a, a, a) cubic cell.

These results are evidence that the determination of the background at $T < T_N$ is satisfactory.

Finally, in order to analyse the $GdBe_{13}$ magnetic structure, we have generalised the Rietveld profile refinement by extending it to incommensurate magnetic structures.

3. Results

3.1. Crystalline structure ($T = 31$ K)

Figure 1 shows the experimental $GdBe_{13}$ nuclear pattern at $T = 31$ K together with the calculated profile. The $Fm3c$ nuclear structure parameters are listed in table 1. The scattering lengths at $\lambda = 0.504$ Å were taken as $b_{Be} = 0.774 \times 10^{-12}$ cm (Bacon 1972) and $b_{Gd} = 1.08(5) \times 10^{-12}$ cm: b_{Gd} was considered as a parameter in the refinement process and the value obtained compares well with $b_{Gd} = 1.1(1) \times 10^{-12}$ cm (Morin *et al* 1978).

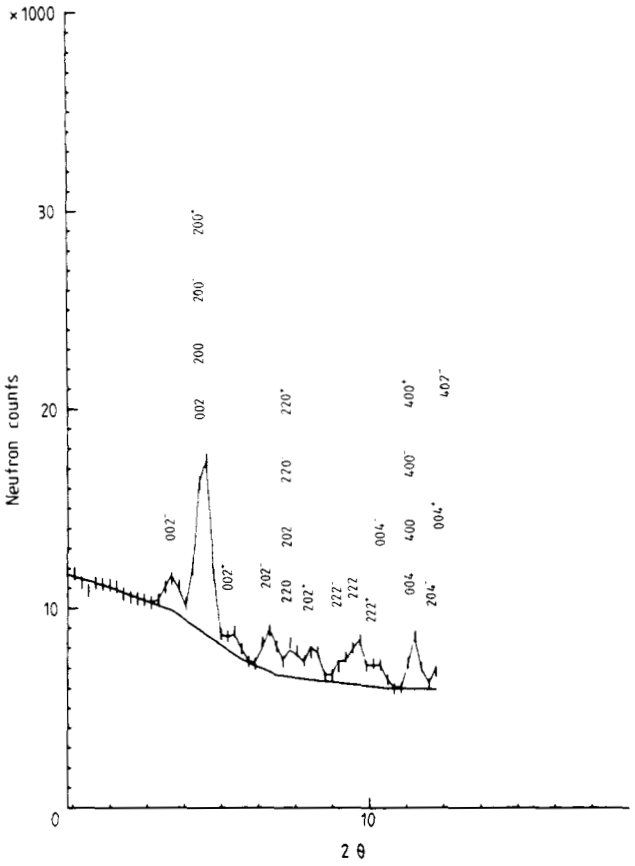

Figure 4. Profile refinement for magnetic structure ($T = 20$ K). The calculated profile (upper full curve) corresponds to an incommensurate magnetic structure with $\tau = 0.29\ c^*$. Nuclear (hkl) and magnetic ($hkl^{\pm}$) Bragg peaks are indexed in the (a, a, a) cubic cell.

Table 1. Nuclear structure of $GdBe_{13}$ at $T = 31$ K (profile refinement results) with

$$R_p = \left(\frac{\Sigma_i w_i [y_i(\text{obs}) - (1/c) y_i(\text{calc})]^2}{\Sigma_i w_i (y_i(\text{obs}))^2} \right)^{1/2}$$

$$R_N = \frac{\Sigma_{\boldsymbol{K}} |F_{\boldsymbol{K}}^2(\text{obs}) - (1/c) F_{\boldsymbol{K}}^2(\text{calc})|}{\Sigma_{\boldsymbol{K}} F_{\boldsymbol{K}}^2(\text{obs})}$$

where $F_{\boldsymbol{K}}$ is the nuclear structure factor for $\boldsymbol{K} = h\boldsymbol{a}^* + k\boldsymbol{b}^* + l\boldsymbol{c}^*$.

Cubic cell parameter	$a = 10.20(1)$ Å
96(i) positional parameters	$y = 0.1155(5)$ $z = 0.1772(4)$
Isotropic Debye parameters	$B_{Gd} = 0.2(3)$ Å^2 $B_{Be} = 1.2(3)$ Å^2
Profile reliability	$R_p = 7.65\%$ $R_N = 3.5\%$

Table 2. Magnetic structure of $GdBe_{13}$ at $T = 20$ K, 12 K and 3 K (profile refinement results) with

$$R_p = \left(\frac{\Sigma_i w_i [y_i(\text{obs}) - (1\ c) y_i(\text{calc})]^2}{\Sigma_i w_i (y_i(\text{obs}))^2} \right)^{1/2}$$

$$R_M = \frac{\Sigma_K | |\boldsymbol{J}_K(\text{obs})|^2 - (1\ c) |\boldsymbol{J}_K(\text{calc})|^2 |}{\Sigma_K |\boldsymbol{J}_K(\text{obs})|^2}$$

where $\boldsymbol{J}_K$ is the magnetic structure factor.

	$T = 20$ K	$T = 12$ K	$T = 3$ K
Magnetic moment, M, per Gd^{3+} unit (μ_B)	5.4(2)	6.1(2)	6.6(1)
Propagation vector, τ	0.290(4) c^*	0.285(3) c^*	0.284(2) c^*
Cubic cell parameter, a (Å)	10.20(2)	10.19(2)	10.25(2)
Background, α (arbitrary unit)	910(50)	1180(50)	1400(50)
Profile reliability (%)			
R_p	7.1	6.5	7.2
R_M	5.5	5.0	4.9

Since, for $\mu R = 1$, the ratio of absorption correction factors at 2θ maximum and minimum values is $A(2\theta_{max} = 24°)/A(2\theta = 0°) = 1.015$ no absorption correction was used. In the experimental conditions $\lambda = 0.504$ Å, $2\theta \leqslant 24°$, $\mu R = 1$, absorption could be accounted for by a negative temperature factor B defined by:

$$A(2\theta)/A(0) = \exp(-2B \sin^2\theta/\lambda^2)$$

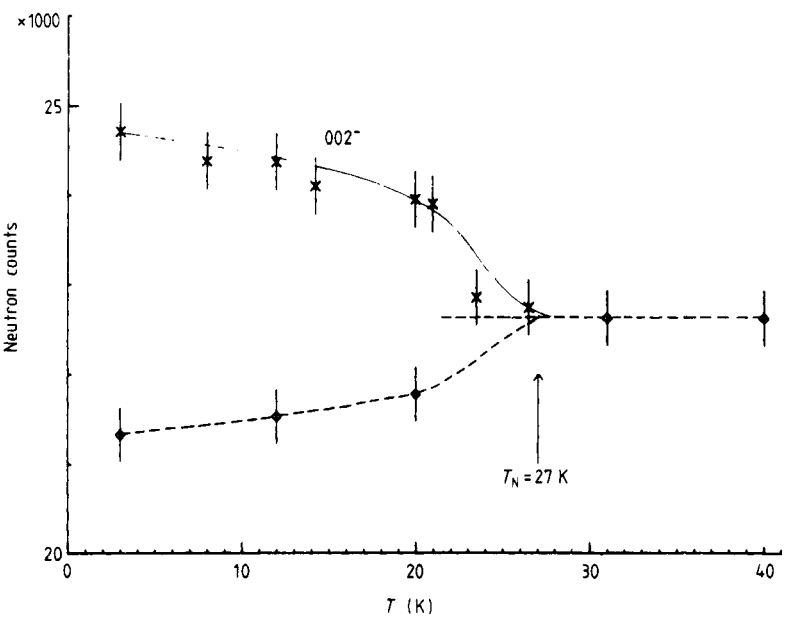

Figure 5. Determination of the Néel temperature T_N of $GdBe_{13}$: (×) observed intensity, (◇) background, at $2\theta = 4.75°$.

and equal to -0.045 Å^2. However the nuclear structure parameters are not sensitive to such a variation in the B factors and, in particular, no significant difference in the results of table 1 is obtained when $B_{Gd} = 0$.

3.2. Magnetic structure at $T = 3$ K

Previous magnetic measurements on $GdBe_{13}$ (Bucher *et al* 1975) showed that $GdBe_{13}$ is antiferromagnetic below $T_N = 25.7$ K. To establish the magnetic structure at $T = 3$ K, both commensurate and incommensurate models were used in the profile refinement. Figure 2(curve B) shows clearly that the commensurate magnetic structure $\tau = c^*/3$ (magnetic cell: $(a, a, 3a)$) does not fit the experimental 2θ reflection positions. In figure 2(curve A) the calculated profile corresponds to an incommensurate spiral structure, with a propagation vector $\tau = 0.284(2)c^*$ and magnetic moments $M = 6.6(1)\ \mu_B$ perpendicular to the c axis.

The magnetic structure factors for $\boldsymbol{K} = (h\boldsymbol{a}^* + k\boldsymbol{b}^* + l\boldsymbol{c}^*) \pm \tau$:

$$|J_{\boldsymbol{K}}|^2 = \frac{1 + \cos^2(\boldsymbol{K}, \boldsymbol{c}^*)}{4} \left| \sum_j 0.27 f M \exp[2i\pi(h\boldsymbol{a}^* + k\boldsymbol{b}^* + l\boldsymbol{c}^*)\cdot \boldsymbol{r}_j \right|^2$$

were calculated with the Gd^{3+} magnetic form factor of Freeman and Desclaux (1979).

3.3. Thermal variation of the magnetic structure

Figures 2, 3 and 4 show $GdBe_{13}$ neutron diffraction patterns at $T = 3$ K, 12 K and 20 K. The results of the profile refinement for the magnetic structure are summarised in table 2.

The propagation vector τ of the spiral structure is independent of temperature. This property allows us to study the thermal variation of the $00\bar{2}^-$ satellite intensity only at $2\theta = 4.75°$ (figure 5).

For $T = 3$ K, 12 K and 20 K the neutron background was estimated from $T = 31$ K as explained before (§2.2). Neutron diffraction determination of the Néel temperature (figure 5) then leads to $T_N = 27 \pm 3$ K, consistent with the value of $T_N = 25.7$ K obtained from susceptibility measurements (Bucher *et al* 1975).

The Gd^{3+} magnetic moments $\boldsymbol{M}$ are perpendicular to the propagation vector of the structure. Figure 6 shows M as a function of T/T_N.

3.4. Molecular field coefficients in $GdBe_{13}$

We shall now discuss magnetic susceptibility and neutron diffraction results in a molecular field approximation. From magnetic susceptibility measurements we can obtain the paramagnetic Curie temperature θ_p. Bucher *et al* (1975) measured $\theta_p = 25$ K for $GdBe_{13}$. From neutron diffraction, we know that $GdBe_{13}$ is helimagnetic below $T_N = 27$ K, with ferromagnetic (001) planes of moments $\boldsymbol{M}$ perpendicular to $\boldsymbol{c}$. Let φ_0 be the angle between magnetic moments in adjacent planes:

$$\varphi_0 = 2\pi\ \tau\cdot\boldsymbol{c}/2 \qquad \tau = 0.285\ \boldsymbol{c}^*.$$

Denoting the molecular field coefficients by J_0 (within each plane), J_1 (between nearest-neighbour planes) and J_2 (between next-nearest-neighbour planes), for an helimagnetic structure, the molecular field H_m may be written as:

$$H_m = (J_0 + 2J_1 \cos\varphi_0 + 2J_2 \cos 2\varphi_0) M$$

where θ_p, T_N and φ_0 are related to J_0, J_1 and J_2 through:

$$\theta_p = C(J_0 + 2J_1 + 2J_2) \tag{1}$$

$$T_N = C(J_0 + 2J_1 \cos\varphi_0 + 2J_2 \cos 2\varphi_0) \tag{2}$$

$$\cos\varphi_0 = -J_1/4J_2 \tag{3}$$

where C denotes the Curie constant of Gd^{3+} ($J = \frac{7}{2}$, $g_J = 2$).

From the experimental results $\theta_p = 25$ K, $T_N = 27$ K, $\tau = 0.285\ c^*$, and from equations (1), (2) and (3) we get:

$$CJ_0 = 14.3\,\text{K} \qquad CJ_1 = 8.9\,\text{K} \qquad CJ_2 = -3.5\,\text{K}.$$

Below the Néel temperatures T_N, the magnetic moment $M = \sigma g_J J$ is given, in the molecular field treatment, as the solution of:

$$\sigma = \mathscr{B}_J\{[3J/(J+1)]\,(T_N/T)\,\sigma\}$$

where $\mathscr{B}_J(x)$ is the Brillouin function. This molecular field prediction (full curve) is shown in figure 6. The agreement between theory and experiment is quite reasonable.

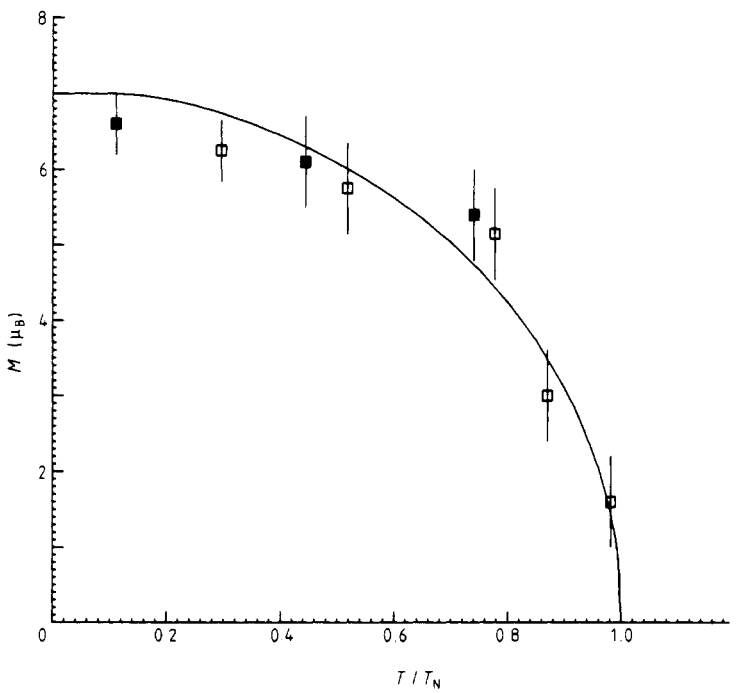

Figure 6. $GdBe_{13}$ magnetic moment (in μ_B per Gd^{3+} ion) as a function of T/T_N. The experimental Gd^{3+} magnetic moment is either deduced from Rietveld profile refinement of a neutron powder pattern (■) or obtained from the thermal variation of the $00\frac{2}{2}^-$ magnetic Bragg peak (□). The experimental error is taken as four Rietveld standard deviations (Sakata and Cooper 1979). The full curve is the molecular field prediction for the magnetic moment for $J = 7\ 2$ and $g_J = 2$.

Bucher *et al* (1975) also studied the influence of an external magnetic field on the $GdBe_{13}$ spin configuration: a non-linear magnetisation behaviour was observed for $H > H_S = 5$ kOe at $T = 1.4$ K.

When a magnetic field is applied to a spiral structure, for sufficiently large fields, one ultimately arrives at a ferromagnetic arrangement. The critical field H_0, for which complete ferromagnetic alignment is observed is (Nagamiya 1967):

$$H_0 = [(T_N - \theta_p)/C]M$$

which gives for $GdBe_{13}$: $H_0 = 10 \pm 10$ kOe for $M = 7\mu_B$ and is based on the relatively large uncertainty in the measured quantity $T_N - \theta_p$. However the transition from spiral to ferromagnetic structure is complex in nature, going through various intermediate steps (Herpin and Meriel 1961, Nagamiya 1967). A precise determination of these steps on $GdBe_{13}$ would require a single crystal: as the experimental results on $GdBe_{13}$ were obtained on polycrystalline samples, we can only say that $H_S = 5$ kOe is not inconsistent with $H_0 \simeq 10$ kOe.

4. Conclusion

The magnetic structure observed in $GdBe_{13}$ at temperatures below T_N is an incommensurate spiral structure, with a propagation vector independent of T. This magnetic structure is determined by exchange interactions only: $GdBe_{13}$ is a compound with negligible magnetocrystalline anisotropy.

The role of anisotropy is evidenced by the magnetic structures observed in $REBe_{13}$ compounds with RE different from Gd. At $T = 0$ K the only observed structure is commensurate (magnetic cell: $(a, a, 3a)$). At higher T an incommensurate structure can be observed (for RE = Tb and Ho) with a propagation vector τ depending on temperature (Vigneron 1981).

A qualitative interpretation can be given. At $T = 0$ K we can argue that the anisotropy is greater than the exchange, thus leading to a commensurate magnetic structure. In the competition between exchange (incommensurate spiral structure of $GdBe_{13}$) and anisotropy (commensurate magnetic structure), the relative importance of the two terms varies with temperature: at T is lowered, the role of anisotropy is increased. It results in a modification of the helimagnetic structure (τ varying with T, distortion of the spiral) followed by a lock-in at the commensurate $\tau = c^*/3$ propagation vector. For RE = Dy and Er, the anisotropy is sufficient at $T = T_N$ to guarantee the commensurate structure.

Acknowledgments

The authors thank Dr P Chieux and S Cummings for help and discussion during the experiment. They are very grateful to Dr P Meriel for critical and helpful comments on their work.

References

Bacon G E 1972 *Acta Crystallogr.* A **28** 357
Bucher E, Maita J P, Hull G W, Fulton R C and Cooper A S 1975 *Phys. Rev.* B **11** 440

Freeman A J and Desclaux J P 1979 *J. Magn. Magn. Mater.* **12** 11
Herpin A and Meriel P 1961 *J. Phys. Radium* **22** 337
Herr A, Besnus M J and Meyer A J P 1975 *Int. Colloques CNRS* **242** 47
Hewat A W 1973 *J. Physique Coll.* C6 2559
Morin P, Pierre J, Schmitt D and Givord D 1978 *Phys. Lett.* **65A** 156
Nagamiya T 1967 *Solid State Phys.* **20** 305 (New York: Academic)
Rietveld H M 1967 *Acta Crystallogr.* **22** 151
Sakata M and Cooper M J 1979 *J. Appl. Crystallogr.* **12** 554
Vigneron F, Sougi M, Meriel P, Herr A and Meyer A 1980 *J. Physique* **41** 123
Vigneron F 1981 *PhD Thesis* University of Paris to be published